Atmos. Chem. Phys. Discuss., 9, 6425–6449, 2009
www.atmos-chem-phys-discuss.net/9/6425/2009/

Atmospheric Chemistry and Physics Discussions

This discussion paper is/has been under review for the journal *Atmospheric Chemistry and Physics (ACP)*. Please refer to the corresponding final paper in *ACP* if available.

In-cloud processes of methacrolein under simulated conditions – Part 2: Formation of Secondary Organic Aerosol

I. El Haddad[1], Y. Liu[1], L. Nieto-Gligorovski[1], V. Michaud[2], B. Temime-Roussel[1], E. Quivet[1], N. Marchand[1], K. Sellegri[2], and A. Monod[1]

[1]Laboratoire Chimie Provence (UMR 6264), Universités d'Aix-Marseille I, II et III – CNRS, 3 place Victor Hugo, 13331 Marseilles Cedex 3, France
[2]Laboratoire de Météorologie Physique (UMR 6016), Observatoire de Physique du Globe de Clermont-Ferrand, Université Blaise Pascal, 24 avenue des Landais, 63177 Aubière, France

Received: 22 January 2009 – Accepted: 5 February 2009 – Published: 10 March 2009

Correspondence to: I. El Haddad (imad.el-haddad@etu.univ-provence.fr)

Published by Copernicus Publications on behalf of the European Geosciences Union.

Abstract

The fate of methacrolein in cloud evapo-condensation cycles was experimentally investigated. To this end, aqueous-phase reactions of methacrolein with OH radicals were performed (as described in Liu et al., 2009), and the obtained solutions were then nebulized and dried into a mixing chamber. The ESI-MS and ESI-MS/MS analyses of the aqueous phase composition denoted the formation of high molecular weight multifunctional products containing hydroxyl, carbonyl and carboxylic acid moieties. The time profiles of these products suggest that their formation can imply radical pathways. These high molecular weight organic products are certainly responsible for the formation of SOA observed during the nebulization experiments. The size, number and mass concentration of these particles increased significantly with the reaction time: after 22 h of reaction, the aerosol mass concentration was about three orders of magnitude higher than the initial aerosol quantity. The evaluated SOA yield ranged from 2 to 12%. This provides, for the first time to our knowledge, strong experimental evidence that cloud processes can act as important contributors to secondary organic aerosol formation in the troposphere. The hygroscopic properties of these secondary organic aerosols are analysed in Michaud et al. (2009).

1 Introduction

Isoprene accounts for about half of all VOC emissions in the atmosphere and is, on a mass basis, the dominant emitted biogenic VOC component with an average global emission of 410 $Tg\,yr^{-1}$ (Muller et al., 2008). Its contribution to SOA budget was believed to be negligible until very recently when heterogeneous pathways were investigated. In this manner, Claeys et al. (2004a, b) measured significant concentrations of tetrols and related species in ambient particle matter, and provided strong evidence that these compounds were formed during the oxidation of isoprene and its first generation oxidation products such as methacrolein. Furthermore, several smog chamber

ACPD

9, 6425–6449, 2009

experiments investigated the SOA formation from isoprene, and reported yields of 1–4% (Edney et al., 2005; Dommen et al., 2006; Kroll et al., 2006; Surratt et al., 2006). They suggested that isoprene and its oxidation products (methacrolein, 3-methylfuran ...) can contribute to ambient SOA by heterogeneous reactions under acidic conditions or through polymerization of second generation oxidation products. Accordingly, Surratt et al. (2006) demonstrated a major contribution of methacrolein in the SOA formation through isoprene reactivity, and proposed particle phase esterification reactions as a major SOA formation pathway. With a global emission rate of 410 Tg yr^{-1}, isoprene is believed to produce, through heterogeneous pathways, substantial amounts of SOA even with low SOA yields (Kanakidou et al., 2005). However, these mechanisms do not take into account those occurring through cloud processes.

Clouds play a major role in atmospheric chemistry, because they strongly affect the chemical composition of the troposphere. The cloud droplets provide an efficient medium for liquid phase reactions of water soluble species, and more than 60% of the total sulfates on a global scale are estimated to be produced from cloud processing (Liao et al., 2003). Recent studies suggest that, as sulfates, SOA can also be produced through aqueous phase reactions in clouds, fogs and aerosols (Blando and Turpin 2000; Ervens et al., 2003, 2004a, b, 2008; Gelencser and Varga, 2005; Lim et al., 2005; Altieri et al., 2006, 2008; Carlton et al., 2006, 2007). Briefly, reactive organics are oxidized in the interstitial spaces of clouds to form highly water-soluble compounds (e.g. aldehydes) that readily partition into the droplets. The dissolved organics may undergo chemical conversions in the aqueous phase (hydrolysis, further oxidation, polymerisation ...), to form less volatile organics. These products remain, at least in part, in the particle phase upon droplet evaporation, leading to SOA mass production (Kanakidou et al., 2005). The results obtained from several experimental studies support the in-cloud SOA hypothesis. Loeffler et al. (2006) demonstrated the formation of SOA through the self-oligomerization of glyoxal and methylglyoxal, when aqueous solutions of these products were evaporated. Likewise, photochemical experiments conducted on pyruvic acid, methylglyoxal, and glyoxal clearly demonstrated

the formation of higher mass products that can potentially participate in SOA production, upon cloud droplets evaporation (Altieri et al., 2006, 2008; Carlton et al., 2006, 2007). Based on these findings, Ervens et al. (2008) have developed a cloud parcel model that supported in-cloud SOA (called SOA_{drop}) formation from isoprene and its oxidation products, and they obtained a carbon yield of SOA_{drop} ranging from 0.4 to 42%.

Methacrolein is a major gas phase reaction product of isoprene (Lee et al., 2005) that was observed in the gas phase and in cloud and fog waters (van Pinxteren et al., 2005). The aim of this study is to investigate the ability of methacrolein to form SOA after in-cloud aqueous phase photooxidation followed by droplets evaporation, and to determine the resulting SOA yield.

2 Experimental section

In order to investigate the fate of methacrolein in cloud water, photochemical aqueous-phase reactions of methacrolein with OH radicals were performed. The aqueous solutions obtained at different reaction times were then nebulized and dried into a mixing chamber, in order to simulate a cloud evaporation process. The number size distribution of the obtained SOA in the mixing chamber was tracked using a SMPS. The aqueous-phase composition was analysed by ESI-MS/MS, in order to investigate the organic species implicated in the production of SOA through cloud processing.

2.1 Aqueous phase reaction

OH-oxidation of methacrolein was studied in an aqueous phase photoreactor (Liu et al., 2009). Briefly, it is a 450 mL Pyrex thermostated reactor, equipped with Xenon arc lamp (300 W; Oriel). The OH radicals were produced by H_2O_2 photolysis. The experiments were performed at 25°C and "free pH" (unbuffured solutions). The initial concentrations of methacrolein and H_2O_2 were 2–5.10^{-3} M and 0.4 M, respectively. The good

reproducibility of aqueous phase OH-oxidation of methacrolein was verified through a series of 9 experiments (Liu et al., 2009). To reach the goals of the present study, a 10th and an 11th experiments were performed in the same conditions, where samples were taken at 0 h, 5 h, 9.5 h, 14 h and 22 h for the aerosol generation experiments.

2.2 Analytical determinations

The ESI-MS and ESI-MS/MS analysis were conducted using a triple quadrupole mass spectrometer (Varian 1200L), equipped with an electrospray ionisation (ESI) chamber. Samples and standard solutions were directly injected (no chromatographic column) into the ESI source region at a flow rate of 25 μL min^{-1}. Two experiments were performed using the coupling of the aqueous phase photoreactor with the mass spectrometer ESI source, following the procedure described in Poulain et al. (2007). The ESI-MS and ESI-MS/MS analysis were performed in both positive and negative modes using the conditions described in Liu et al. (2009).

In addition, samples taken at different reaction times were analysed by HPLC-APCI-MS/MS (Varian 1200L). The separation column was a Synergi Hydro-RP 250×2.4 μm, Phenomenex. The analytes were chromatographically resolved using a gradient of 2 solvents (A: 0.1% acetic acid aqueous solution and B: methanol) delivered at a constant flow rate of 0.2 mL min^{-1}, with A:B=95%:5% from 0 to 12 min and 0%:100% at 60 min during 5 min. The analysis was realized using single ion monitoring (SIM) in the negative and the positive ionisation modes of the APCI, at −40 V and +40 V, respectively. The nebulising gas was synthetic air for the negative mode and nitrogen for the positive mode. It was delivered at a pressure of 55 psi at a temperature of 300°C. Nitrogen served both as the drying gas and the auxiliary gas at a pressure of 15 and 3 psi, respectively. The temperature of the drying gas was held at 350°C.

2.3 Aerosol generation and characterisation

The experimental setup used for the aerosol generation experiments is presented in Fig. 1. During these experiments, liquid samples taken from the photoreactor at specific reaction times were nebulised, using a TSI 3079 atomizer, in order to generate sub-micrometer water droplets. The atomizer flow rate was fixed at 4.2 L min^{-1}. The generated water droplets were then dried by mixing with pure dry air at a flow rate of 5 L min^{-1} and passing through a silica gel diffusion dryer. After drying, the aerosol was delivered into a 200 L Teflon (PTFE) mixing chamber. At these operating conditions, the average residence time of the aerosol in the whole setup was about 20 min, and the resulting relative humidity was 20–30% in the mixing chamber (Fig. 1). The aerosols obtained at different aqueous phase reaction times were characterised in term of their number size distributions and their hygroscopicity and volatility. The size distribution of the generated aerosol was monitored using a Scanning Mobility Particle Sizer (SMPS) connected to the mixing chamber (Fig. 1). The SMPS is composed of a long column Differential Mobility Analyzer (L-DMA, GRIMM Inc.) and a Condensation Particle Counter (CPC, model 5.403, GRIMM Inc.). The DMA aerosol and sheath operating flow rates were 0.3 and 3 L min^{-1}, respectively. These settings allowed for a particle sampling range from 11.1 to 1083 nm, within 6 min 46 s. The aerosol hygroscopicity and volatility measurements were conducted using a Volatility Hygroscopicty Tandem DMA (HVTDMA) (Fig. 1); the experimental procedure and the results dealing with these measurements are reported in Michaud et al. (2009). Before each nebulisation experiment, the mixing chamber was flushed for about 2 h (~6 times) with synthetic air, and aerosol blanks were controlled by SMPS measurements prior to each new experiment. For each experiment, the particles size distributions were recorded after 1 h of nebulisation and during approximately 2 h. Average distributions were then determined for each reaction time.

ACPD
9, 6425–6449, 2009

3 Results and discussion

3.1 Aqueous phase characterisation

As described in Liu et al. (2009), during the aqueous phase reaction, 70% of methacrolein was consumed within 10 h. Several reaction products were identified and quantified, including formaldehyde, formic acid, acetic acid, methylglyoxal, hydroxyacetone, oxalic acid, glyoxylic acid, methacrylic acid, peroxymethacrylic acid, 2-hydroxy-2-methylmalonaldehyde, 2,3-dihydroxy-2-methylpropanal, 2-methylglyceric acid, pyruvic acid and dihydroxymethacrylic acid. The chemical mechanism associated to these products is discussed in Liu et al. (2009). The authors reported a significant lack in the carbon balance of up to 45%, which is related to unidentified reaction products. A thorough study of the ESI-MS spectra at different reaction times show a large number of high molecular weight ions in both the positive and the negative modes, which can explain this lack of carbon. The resulting spectra are illustrated as a function of the reaction time in Fig. 2. The most abundant ions in both modes cluster in the mass range of 100–250 amu and some ions up to 320 amu are also observed. over 400 amu no ions were observed under our instrumental conditions. Similar ESI-MS distribution patterns had been reported previously by Altieri et al. (2006, 2008), during the aqueous phase photooxidation of pyruvic acid and methylglyoxal. This distribution appears to be consistent with the development of an oligomer system that shows a highly regular pattern of mass differences of 12, 14, 16 and 18 amu (Altieri et al., 2006, 2008; Poulain et al., 2007). In the present study, Fig. 3 shows that the observed ions were not detected in the spectra of standard mixtures containing methacrolein, formaldehyde, methylglyoxal, hydroxyacetone, formic, acetic, pyruvic, oxalic, glyoxylic and methacrylic acids, even at concentrations representative of the reaction sample at 20 h. This suggests that the observed oligomer formation is not an analytical artefact occurring during the electrospray ionisation, i.e. adducts formed in the ionisation chamber by the combination of smaller molecules.

Figures 2 and 3 show the complex nature of the matrix and the complexity of the

mechanisms behind the formation of these products. The complexity in the ESI-MS spectra occurs in both the positive and negative modes, thus indicating that the oligomers formed in the aqueous phase are most likely multifunctional compounds. The observed MS compounds were further characterized for their MS/MS fragmentation in order to elucidate their chemical structures. The MS/MS patterns allowed us to group these compounds into two remarkable series: series A in the negative mode and series B in the positive mode (Table 1). In these series, each parent ion exhibits in its MS/MS spectra at least one daughter ion corresponding to another parent ion of the same series. This suggests that, in each series, the compounds associated to the parent ions include in their structure the same structural units, thus significantly denoting the formation of oligomers. For each series, the HPLC-APCI-MS analysis showed that the parent ions had different retention times, which attribute them to different reaction products. A detailed discussion of the HPLC-MS analysis of each series is presented hereafter.

– In series A (Fig. 4), the smallest ions, (*m/z* 73^- and 87^-) are related, respectively, to glyoxylic and pyruvic acids, which are secondary oxidation products of methacrolein (Liu et al., 2009). This series also exhibits two higher molecular weight ions, *m/z* 143^- and 187^- The chromatogram associated with *m/z* 187^- exhibits a sharp peak at 28.6 min and a smaller peak at a longer retention time (37.4 min) (Fig. 4b), thus corresponding to two different compounds having the same molecular mass of 188 g mol^{-1}. The collision-induced dissociation of *m/z* 187^- mainly leads to two predominent daughter ions at *m/z* 143^- and 87^- (Table 1). The *m/z* 143^- daughter ion, resulting from the loss of CO_2 as a neutral fragment (44 uma), indicates the presence of at least one carboxylic acid functional group (Dron et al., 2007). The *m/z* 87^- daughter ion suggests that at least one of the two products associated with *m/z* 187^- include in its chemical structure the pyruvate as a structural subunit. The HPLC-MS chromatogram of *m/z* 143^- exhibits two peaks at 26.50 and 35.44 min (Fig. 4b), which can, also, be attributed to two different compounds. The MS/MS analysis of *m/z* 143^- exhibits,

among others, daughter ions of *m/z* 73^- and 87^- thus denoting the presence of the glyoxylate or the pyruvate as a structural subunit. The MS/MS fragmentation patterns and the high retention times of *m/z* 143^- and 187^- of series A, clearly, associate them to high molecular weight multifunctional compounds, produced probably from the reaction of pyruvic acid. The contribution of pyruvic acid to the formation of oligomers through aqueous phase oxidation was previously observed by Altieri et al. (2006, 2008) and Guzman et al. (2006). However, it should be noted that these authors proposed different reaction pathways in order to explain the oligomer formation: Altieri et al. (2006, 2008) suggest molecular (esterification) additions of smaller compounds including pyruvic acid, glyoxylic acid, and oxalic acid; whereas Guzman et al. (2006) proposed a radical mechanism. In the present study, the data presented do not permit the determination of the reaction pathways for the products of series A.

– In series B (Fig. 5), the HPLC-MS chromatograms associated with the parent ions indicate that they are, apparently, related to a complex mixture of numerous compounds and isomers. The chromatograms of *m/z* 137^+, 155^+ and 173^+ exhibit more than five resolved peaks and a broad peak at a retention time of ~27 min. The chromatograms associated with *m/z* 197^+ and 201^+ do not show any peak, which suggests that the corresponding compounds were not eluted under our conditions (Fig. 5). These chromatographic aspects can be attributed to the high molecular weight and the multifunctional nature of the compounds associated with this series. Likewise, the collision-induced dissociation of *m/z* 109^+, 127^+, 137^+, 155^+, 173^+, 197^+ and 201^+ frequently yields neutral losses of H_2O (18 uma), CO (28 uma), H_2O + CO (46 uma) and 2×CO (56 uma) (Table 1) which relate them to hydroxyl and carbonyl moieties: hydroxy-carbonyl or carboxylic acids and confirm their multifunctional nature. The time profiles of the intensities of *m/z* 109^+, 127^+, 137^+, 155^+, 173^+, 197^+ and 201^+ as a function of consumed methacrolein (Fig. 5a) shows direct formation (with no time delay). This pattern indicates that the corresponding compounds are first generation (primary) prod-

ucts. In the present study, the fact that the oligomer series B corresponds to primary reaction products points out that the oligomer formation bypasses the primary stable oxidation products and includes only methacrolein as a reaction substrate. It is thus likely that the oligomerization mechanism for this series proceeds via radical mechanisms in good agreement with the mechanism pathways proposed by Guzman et al. (2006), rather than ionic or molecular additions (such as esterification, aldol condensation and acetylation). This mechanism occurs somehow through the combination of the radicals formed from the OH-oxidation of methacrolein with another methacrolein molecule or another first generation radical. The multiple additions of different primary radicals may explain the different first generation high molecular weigh products associated to the fragments observed in series B.

In series B, after ~5 h of reaction, the intensity of most of the ions reached a plateau or started to decrease. This can be attributed to further reaction of the corresponding compounds, thus showing that the formed oligomers can be sensible to photochemistry. The degradation of higher mass compounds was previously observed during the aqueous phase OH-oxidation of glyoxal (Carlton et al., 2007). The authors suggested this degradation as a possible pathway for the formation of smaller non volatile organic acids, such as oxalic acid. Thus, these smaller compounds were secondary products, in good agreement with our observations in series A.

3.2 SOA formation

Considering the molecular mass range and the functionality of the aqueous phase products observed in Sect. 3.1, these compounds are believed to be particularly low volatile. The ability of these compounds to produce SOA upon water droplets evaporation was experimentally examined by nebulising and drying the reaction samples, using the setup described in Fig. 1. The results clearly show a significant production of SOA (Fig. 6). This figure shows a clear evolution of the particle size distributions with

the reaction time. At the initial reaction time (0 min), the aerosol size distribution was determined by nebulizing an aqueous mix of the reactants (methacrolein+H_2O_2). This experience was repeated 3 times and the generated aerosol had an average mass concentration ($M_{0\,h}$) of 0.03 $\mu g\,m^{-3}$ (Table 2), assuming a particle density of 1 $g\,cm^{-3}$. This concentration value was not statistically different from the one measured for the aerosol generated by nebulizing a pure water solution (18 $m\Omega\,cm$) (T-test 0.05 level; Sokal and Rohlf, 1981). These results support the fact that methacrolein is highly volatile, and thus, is not able to produce particles. After 5 h of aqueous phase reaction, the aerosol quantity was low ($M_{5\,h}$=1.4 $\mu g\,m^{-3}$), but significantly higher than $M_{0\,h}$. Between 5 h and 9.5 h, a substantial increase of the aerosol mass concentration was observed. After 14 h, the aerosol quantity increased steadily as a function of the aqueous-phase reaction time. At 22 h, the aerosol mass concentration reached 27.8 $\mu g\,m^{-3}$, about three orders of magnitude higher than the initial aerosol quantity. Similarly, a significant increase of the aerosol diameter and number was observed: from 0 to 22 h, the aerosol number and diameter have increased by a factor of 254 and 3.7, respectively (Table 2). This evolution clearly demonstrates the ability of the aqueous phase processes to produce particles upon water droplets evaporation. This production can be attributed to the low volatile organic species formed during the aqueous phase OH-oxidation of methacrolein (Sect. 3.1) which remain in the particle phase upon water evaporation, and thus forms the observed SOA. Among the products identified by Liu et al. (2009), such as dihydroxymetharylic acid (Claeys et al., 2004a, b) and oxalic acid (Sempéré and Kawamura, 1996; Kawamura and Sakaguchi, 1999) are low volatile compounds and can contribute at least in part to the SOA mass. Other products, such as methylglyoxal (also identified by Liu et al., 2009), were previously reported (Loeffler et al., 2006; Paulsen et al., 2006) to potentially form low volatility compounds through reactive pathways during droplets evaporation and products accretion. Therefore, it may contribute to the SOA mass. In addition to these compounds, the unidentified high molecular weight multifunctional compounds are believed to be sufficiently low volatile to remain predominantly in the particle phase upon water droplets evaporation.

ACPD
9, 6425–6449, 2009

3.3 SOA mass yield and atmospheric implications

In order to determine the SOA mass yield, we have evaluated the particle losses in our experimental setup. This estimation was determined on the basis of four nebulization experiments of aqueous solutions containing NaCl at 100 mg L^{-1} using the experimental setup described in Fig. 1. The results have shown that the particles transmission efficiency from our system was only 11.3±2.5%. This low efficiency may be due to the experimental set up which contains a guard flask and a small mixing chamber, made of Teflon, which is highly electrostatic. Assuming the same loss for organic particles, we used this value to evaluate the SOA mass yield. This yield was calculated at each reaction time as the ratio between the amount of SOA formed in mg per L of evaporated water and the consumed methacrolein in mg per L of evaporated water (Table 2). The obtained amount of SOA (14–33 mg L^{-1} for reaction times 9.5–22 h) is in good agreement (within the uncertainties) with the values by Michaud et al. (2009) (19–41 mg L^{-1} for reaction times 9.5–22 h) who performed an independent calculation based on volatility measurements. The mass yield depends on the reaction time, but a global yield of 2–12% can be assessed (Table 2). This global yield is higher than the 1–4% mass yield of SOA formed through direct photooxidation of isoprene in the gas phase, and thus, it should enhance the total mass of SOA formed from isoprene in the atmosphere.

4 Conclusion

This work reports an experimental study of the aqueous phase OH-oxidation of methacrolein and the fate of the reaction products upon water droplets evaporation. The aqueous phase reaction products were characterized using ESI-MS, ESI-MS/MS and HPLC-APCI-MS. Several low volatile compounds, including oxalic acid and dihydroxymethacrilic acid, were formed along with other unidentified higher molecular weight multifunctional products. The HPLC-APCI-MS and the MS/MS analyses of the

ACPD
9, 6425–6449, 2009

unidentified products associate them to multiple isomers containing carboxylic acids, oxo-carboxylic acids and hydroxy-carbonyls functions. They also show that some of these reaction products can be assimilated to oligomers. The time profiles of these products point out that their formation can involve radical mechanisms. The ability of these compounds to produce SOA upon water droplets evaporation was, for the first time to our knowledge, experimentally examined by nebulizing and drying the reaction samples, in order to simulate a cloud evaporation process. The results clearly showed a significant production of SOA. A clear evolution of the particle size distributions with the reaction time was obtained: an increase of the aerosol mass from 0.03 $\mu g\,m^{-3}$ to 27.8 $\mu g\,m^{-3}$, within 22 h of reaction was observed. A SOA mass yield of 2–12% was obtained. Our results have experimentally evidenced that cloud processes of methacrolein can produce significant amounts of SOA. Finally, because methacrolein is one of the major oxidation products of isoprene, which is the main emitted VOC on the global scale, it can be anticipated that the in-cloud processes can form significant amounts of SOA, which previously have not been taken into account for a global estimation of SOA atmospheric impacts.

Acknowledgements. This study was funded by the French PN-LEFE-CHAT (Programme National-Les Enveloppes Fluides et l'Environnement-Chimie Atmosphérique), by the Provence-Alpes-Côte-d'Azur Region, and by the French ERICHE network.

References

Altieri, K. E., Carlton, A. G., Lim, H., Turpin, B. J., and Seitzinger, S. P.: Evidence for Oligomer Formation in Clouds: Reactions of Isoprene Oxidation Products, Environ. Sci. Technol., 40, 4956–4960, 2006.

Altieri, K. E., Seitzinger, S. P., Carlton, A. G., Turpin, B. J., Klein, G. C., and Marshall, A. G.: Oligomers formed through in-cloud methylglyoxal reactions: Chemical composition, properties, and mechanisms investigated by ultra-high resolution FT-ICR mass spectrometry, Atmos. Environ., 42, 1476–1490, 2008.

Blando, J. D. and Turpin, B. J.: Secondary organic aerosol formation in cloud and fog droplets: a literature evaluation of plausibility, Atmos. Environ., 34, 1623–1632, 2000.

Carlton, A. G., Turpin, B. J., Lim, H., Altieri, K. E., and Seitzinger, S.: Link between isoprene and secondary organic aerosol (SOA): pyruvic acid oxidation yields low volatility organic acids in clouds, Geophys. Res. Lett., 33, L06822/1–L06822/4, doi:10.1029/2005GL025374, 2006.

Carlton, A. G., Turpin, B. J., Altieri, K. E., Seitzinger, S., Reff, A., Lim, H., and Ervens, B.: Atmospheric oxalic acid and SOA production from glyoxal: Results of aqueous photooxidation experiments, Atmos. Environ., 41, 7588–7602, 2007.

Claeys, M., Graham, B., Vas, G., Wang, W., Vermeylen, R., Pashynska, V., Cafmeyer, J., Guyon, P., Andreae, M. O., Artaxo, P., and Maenhaut, W.: Formation of Secondary Organic Aerosols Through Photooxidation of Isoprene, Science, 303, 1173–1176, 2004a.

Claeys, M., Wang, W., Ion, A. C., Kourtchev, I., Gelencser, A., and Maenhaut, W.: Formation of secondary organic aerosols from isoprene and its gas-phase oxidation products through reaction with hydrogen peroxide, Atmos. Environ., 38, 4093–4098, 2004b.

Dommen, J., Metzger, A., Duplissy, J., Kalberer, M., Alfarra, M. R., Gascho, A., Weingartner, E., Prevot, A. S. H., Verheggen, B., and Baltensperger, U.: Laboratory observation of oligomers in the aerosol from isoprene/NO_x photooxidation, Geophys. Res. Lett., 33, L13805/1–L13805/5, doi:10.1029/2006GL026523, 2006.

Dron, J., Eyglunent, G., Temime-Roussel, B., Marchand, N., and Wortham, H.: Carboxylic acid functional group analysis using constant neutral loss scanning-mass spectrometry, Analytica Chimica Acta, 605, 61–69, 2007.

Edney, E. O., Kleindienst, T. E., Jaoui, M., Lewandowski, M., Offenberg, J. H., Wang, W., and Claeys, M.: Formation of 2-methyl tetrols and 2-methylglyceric acid in secondary organic aerosol from laboratory irradiated isoprene/NOX/SO2/air mixtures and their detection in ambient $PM_{2.5}$ samples collected in the eastern United States, Atmos. Environ., 39, 5281–5289, 2005.

Ervens, B., George, C., Williams, J. E., Buxton, G. V., Salmon, G. A., Bydder, M., Wilkinson, F., Dentener, F., Mirabel, P., Wolke, R., and Herrmann, H.: CAPRAM2.4 (MODAC mechanism): An extended and condensed tropospheric aqueous phase mechanism and its application, J. Geophys. Res., 108(D14), 4426, doi:10.1029/2002JD002202, 2003.

Ervens, B., Feingold, G., Frost, G. J., and Kreidenweis, S. M.: A modelling study of aqueous production of dicarboxylic acids, Part 1: Chemical pathways and organic mass production, J. Geophys. Res., 109, D15205, doi:10.1029/2003JD004387, 2004a.

Ervens, B., Feingold, G., Clegg, S. L., and Kreidenweis, S. M.: A modelling study of aqueous production of dicarboxylic acids, Part 2: Impact on cloud microphysics, J. Geophys. Res., 109, D15206, doi:10.1029/2003JD004575, 2004b.

Ervens, B., Carlton, A. G., Turpin, B. J., Altieri, K. E., Kreidensweis, S. M., and Feingold, G.: Secondary organic aerosol yields from cloud-processing of isoprene oxidation products, Geophys. Res. Lett., 35, L02816/1–L02816/5, doi:10.1029/2007GL031828, 2008.

Gelencsér, A. and Varga, Z.: Evaluation of the atmospheric significance of multiphase reactions in atmospheric secondary organic aerosol formation, Atmos. Chem. Phys., 5, 2823–2831, 2005, http://www.atmos-chem-phys.net/5/2823/2005/.

Guzmán, M. I., Colussi, A. I., and Hoffmann, M. R.: Photoinduced oligomerization of aqueous pyruvic acid, J. Phys. Chem. A, 110, 3619–3626, 2006.

Kanakidou, M., Seinfeld, J. H., Pandis, S. N., Barnes, I., Dentener, F. J., Facchini, M. C., Van Dingenen, R., Ervens, B., Nenes, A., Nielsen, C. J., Swietlicki, E., Putaud, J. P., Balkanski, Y., Fuzzi, S., Horth, J., Moortgat, G. K., Winterhalter, R., Myhre, C. E. L., Tsigaridis, K., Vignati, E., Stephanou, E. G., and Wilson, J.: Organic aerosol and global climate modelling: a review, Atmos. Chem. Phys., 5, 1053–1123, 2005, http://www.atmos-chem-phys.net/5/1053/2005/.

Kawamura, K. and Sakaguchi, F.: Molecular distributions of water soluble dicarboxylic acids in marine aerosols over the Pacific Ocean including tropics, J. Geophys. Res., 104(D3), 3501–3509, 1999.

Kroll, J. H., Ng, N. L., Murphy, S. M., Flagan, R. C., and Seinfeld, J. H.: Secondary Organic Aerosol Formation from Isoprene Photooxidation, Environ. Sci. Technol., 40, 1869–1877, 2006.

Lee, W., Baasandorj, M., Stevens, P. S., and Hites, R. A.: Monitoring OH-Initiated Oxidation Kinetics of Isoprene and Its Products Using Online Mass Spectrometry, Environ. Sci. Technol., 39, 1030–1036, 2005.

Liao, H., Adams, P. J., Seinfeld, J. H., Mickley, L. J., and Jacob, D. J.: Interactions between tropospheric chemistry and aerosols in a unified GCM simulation, J. Geophys. Res., 108(D1), 4001, doi:10.1029/2001JD001260, 2003.

Lim, H., Carlton, A. G., and Turpin, B. J.: Isoprene forms secondary organic aerosol through cloud processing: model simulations, Environ. Sci. Technol., 39, 4441–4446, 2005.

Liu, Y., El Haddad, I., Scarfogliero, M., Nieto-Gligorovski, L., Temime-Roussel, B., Quivet, E.,

Marchand, N., Piquet-Varrault, B., and Monod, A.: In-cloud processes of methacrolein under simulated conditions – Part 1: aqueous phase photooxidation, Atmos. Chem. Phys. Discuss., 9, 6397–6424, 2009, http://www.atmos-chem-phys-discuss.net/9/6397/2009/.

Loeffler, K. W., Koehler, C. A., Paul, N. M., and De Haan, D. O.: Oligomer formation in evaporating aqueous glyoxal and methyl glyoxal solutions, Environ. Sci. Technol., 40, 6318–6323, 2006.

Michaud, V., Sellegri, K., Laj, P., Villani, V., Picard, D., El Haddad, I., Liu, Y., Marchand, N., and Monod, A.: In-cloud processes of methacrolein under simulated conditions-part 3: hygroscopic and volatility properties of the formed secondary organic aerosol, Atmos. Chem. Phys. Discuss., 9, 6451–6482, 2009, http://www.atmos-chem-phys-discuss.net/9/6451/2009/.

Monod, A., Chebbi, A., Durand-Jolibois, R., and Carlier, P.: Oxidation of methanol by hydroxyl radicals in aqueous solution under simulated cloud droplet conditions, Atmos. Environ., 34, 5283–5294, 2000.

Müller, J.-F., Stavrakou, T., Wallens, S., De Smedt, I., Van Roozendael, M., Potosnak, M. J., Rinne, J., Munger, B., Goldstein, A., and Guenther, A. B.: Global isoprene emissions estimated using MEGAN, ECMWF analyses and a detailed canopy environment model, Atmos. Chem. Phys., 8, 1329–1341, 2008, http://www.atmos-chem-phys.net/8/1329/2008/.

Paulsen, D., Weingartner, E., Alfarra, M. R., and Baltensperger, U.: Volatility measurements of photochemically and nebulizer-generated organic aerosol particles, J. Aerosol Sci., 37, 1025–1051, 2006.

Poulain, L., Monod, A., and Wortham, H.: Development of a new on-line mass spectrometer to study the reactivity of soluble organic compounds in the aqueous phase under tropospheric conditions: Application to OH-oxidation of N-methylpyrrolidone, J. Photochem. Photobio. A-Chem., 187, 10–23, 2007.

Sempere, R. and Kawamura, K.: Low molecular weight dicarboxylic acids and related polar compounds in the remote marine rain samples collected from western Pacific, Atmos. Environ., 30, 1609–1619, 1996.

Sokal, R. R. and Rohlf, F. J.: Biometry, 2 ed., Freeman: New York, 1981.

Surratt, J. D., Murphy, S. M., Kroll, J. H., Ng, N. L., Hildebrandt, L., Sorooshian, A., Szmigielski, R., Vermeylen, R., Maenhaut, W., Claeys, M., Flagan, R. C., and Seinfeld, J. H.: Chemical

Composition of Secondary Organic Aerosol Formed from the Photooxidation of Isoprene, J. Phys. Chem. A, 110, 9665–9690, 2006.

van Pinxteren, D., Plewka, A., Hofmann, D., Mueller, K., Kramberger, H., Svrcina, B., Baechmann, K., Jaeschke, W., Mertes, S., Collett, J. L., and Herrmann, H.: Schmuecke hill cap cloud and valley stations aerosol characterisation during FEBUKO (II): Organic compounds, Atmos. Environ., 39, 4305–4320, 2005.

Table 1. MS/MS fragmentations of some observed parent ions, in the negative (series A) and the positive mode (series B).

Ion series	Parent ion (amu)[a]	Daughter ions[a]	Neutral losses[b]
		Negative mode	
A	187^{-} [d]	169^{-} 159^{-} **143^{-}** 125^{-} **87^{-}**	18 28 44 56 62
	143^{-} [d]	125^{-} 99^{-} 97^{-} **87^{-}** 85^{-} **73^{-}** 57^{-}	18 28 30 44 46 56
	87^{-} (pyruvic acid)[d]	43^{-}	44
	73^{-} (glyoxylic acid)[d]	45^{-}	28
		Positive mode	
B	201^{+} [c]	183^{+} 165^{+} **155^{+}** 95^{+}	18 28 36 46 60 70 88
	197^{+} [c]	179^{+} **109^{+}** 95^{+} 85^{+}	18 70 94 102
	173^{+} [c]	**155^{+}** 139^{+} **127^{+}** **109^{+}**	18 28 30 46 64
	155^{+} [c]	**137^{+}** **127^{+}** 113^{+} **109^{+}** 95^{+} 81^{+}	18 28 46 56 60 74
	137^{+} [c]	**109^{+}** 95^{+} 81^{+} 43^{+}	28 56
	127^{+} [c]	**109^{+}** 99^{+} 85^{+} 83^{+} 81^{+} 43^{+}	18 28 46 56
	109^{+} [c]	81^{+} 79^{+}	28 30

[a] the ions in bold were observed both as parent ions (formed during the reaction) and daughter ions.
[b] neutral losses can correspond to : 18 (H_2O); 28 (CO); 30 (HCHO); 36 ($2\times H_2O$); 44 (CO_2); 46 (H_2O+CO); 56 ($2\times$CO); 60 (CH_3COOH); 62 (CO_2+H_2O); 88 ($2\times CO_2$).
[c] Time profile corresponding to a primary reaction product.
[d] Time profile corresponding to a secondary or tertiary reaction product.

ACPD
9, 6425–6449, 2009

Table 2. Characteristics of the aerosol formed by the nebulization of the aqueous solutions obtained at different reaction times. The values reported are the average of multiple SMPS measurements, and the errors indicated are the standard deviation on these averages.

Reaction time	N[a] ($\times 10^3$ cm^{-3})	D_P^b (nm)	M[c] (μg m^{-3})	ΔMACR[d] (μg mL^{-1})	SOA[e] (μg mL^{-1})	Yield[f] (%)
0 h	1±4	13.4±1.7	0.03±0.02	0	0.04±0.01	0
5 h	45±7	17.3±3.8	1.4±0.3	130±13	1.87±0.70	1.6±0.7
9.5 h	163±30	41.1±2.1	10.5±2.2	205±21	14.3±4.9	7.6±3.1
14 h	205±22	46.1±2.4	17.5±3.3	254±25	23.8±8.1	10.2±4.2
22 h	254±20	49.8±3.3	27.8±5.0	304±30	32.7±11.1	11.7±5.3

[a] Total number of aerosol generated by the nebulization of the aqueous solutions obtained at different reaction times.
[b] Particle diameter mode.
[c] Aerosol mass concentration measured by the SMPS assuming a particle density of 1 g cm^{-3}.
[d] Methacrolein consummation during the aqueous phase reaction.
[e] SOA aqueous phase concentrations calculated using the SOA mass concentration determined by SMPS and the particles transmission efficiency evaluated by the nebulisation of a NaCl aqueous solution at 100 mg L^{-1}.
[f] SOA yield calculated for each reaction time as the ratio of the SOA concentrations over the methacrolein consummation.

ACPD
9, 6425–6449, 2009

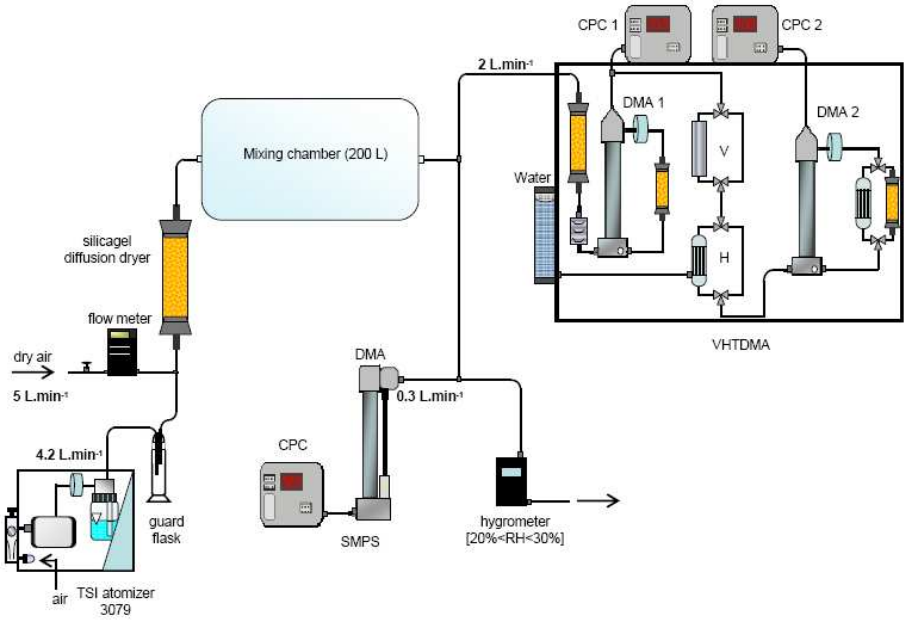

Fig. 1. Scheme of the experimental setup for aerosol generation.

ACPD
9, 6425–6449, 2009

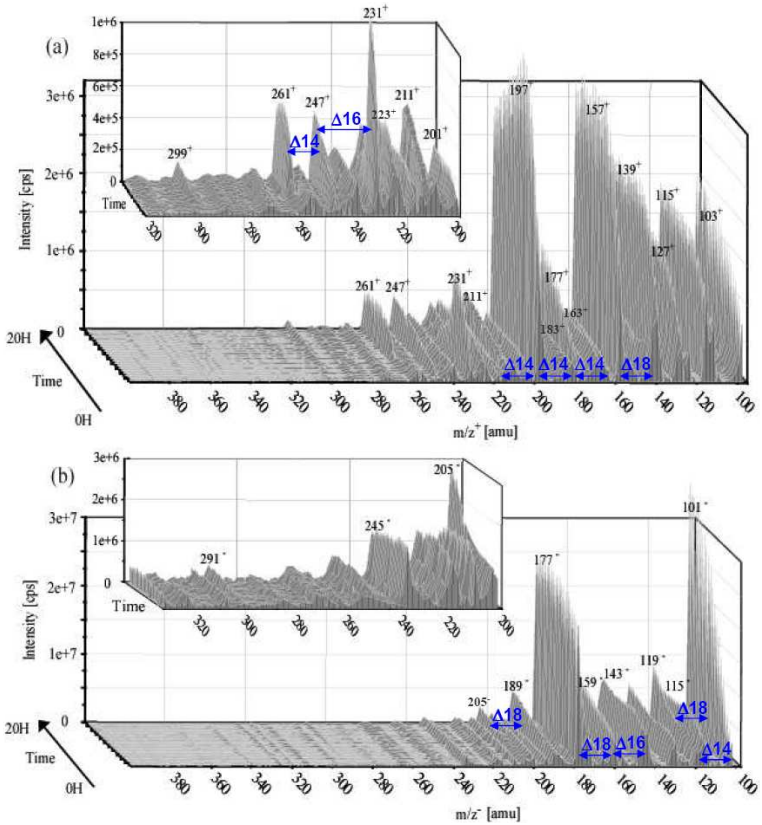

Fig. 2. 3-D time profiles of the mass spectra obtained by ESI/MS analysis from 100 to 400 amu, during the aqueous phase OH-oxidation of methacrolein. **(a)** in the positive mode; **(b)** in the negative mode. For each mode, a zoom from 200 to 320 amu is shown.

ACPD
9, 6425–6449, 2009

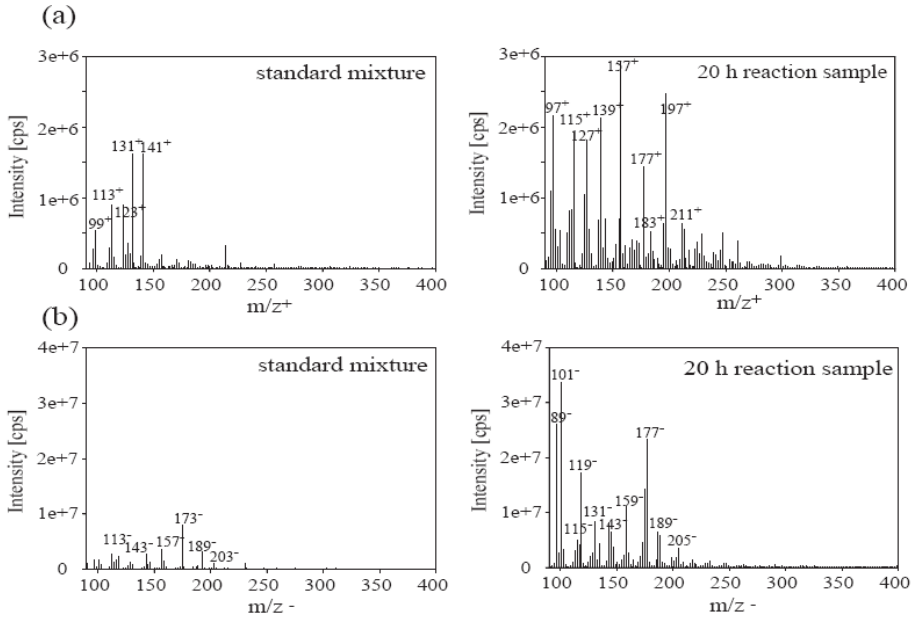

Fig. 3. Comparison of the mass spectra between the standard mixture and a sample after 20 h of reaction **(a)** in the positive mode **(b)** in the negative mode. The standard mixture contains methacrolein (3.10^{-3} M); formaldehyde, methylglyoxal, hydroxyacetone, formic and acetic acids (6.10^{-4} M); pyruvic, oxalic, glyoxylic and methacrylic acids (3.10^{-5} M).

ACPD
9, 6425–6449, 2009

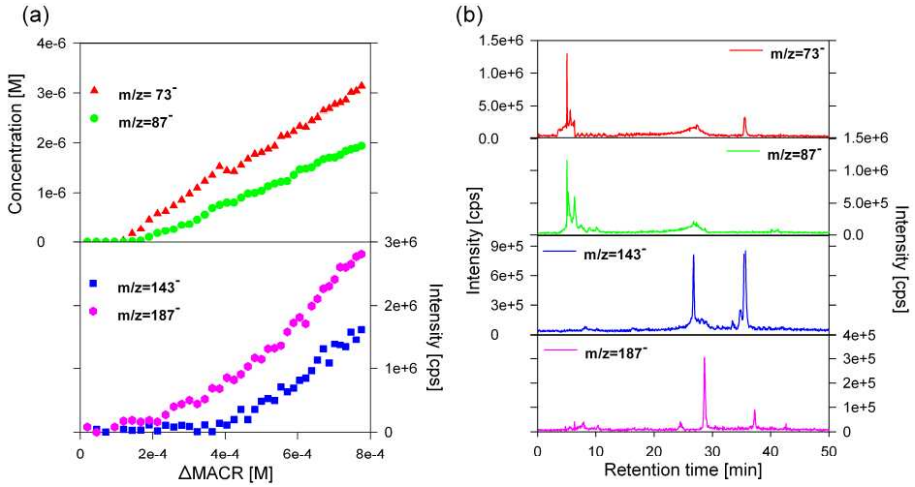

Fig. 4. Characteristics of the oligomer series A. **(a)** Evolution the MS fragments intensities from the series A, along with the concentration of the glyoxilic and the pyruvic acid. **(b)** HPLC chromatographic profiles of the different fragments from the series.

ACPD
9, 6425–6449, 2009

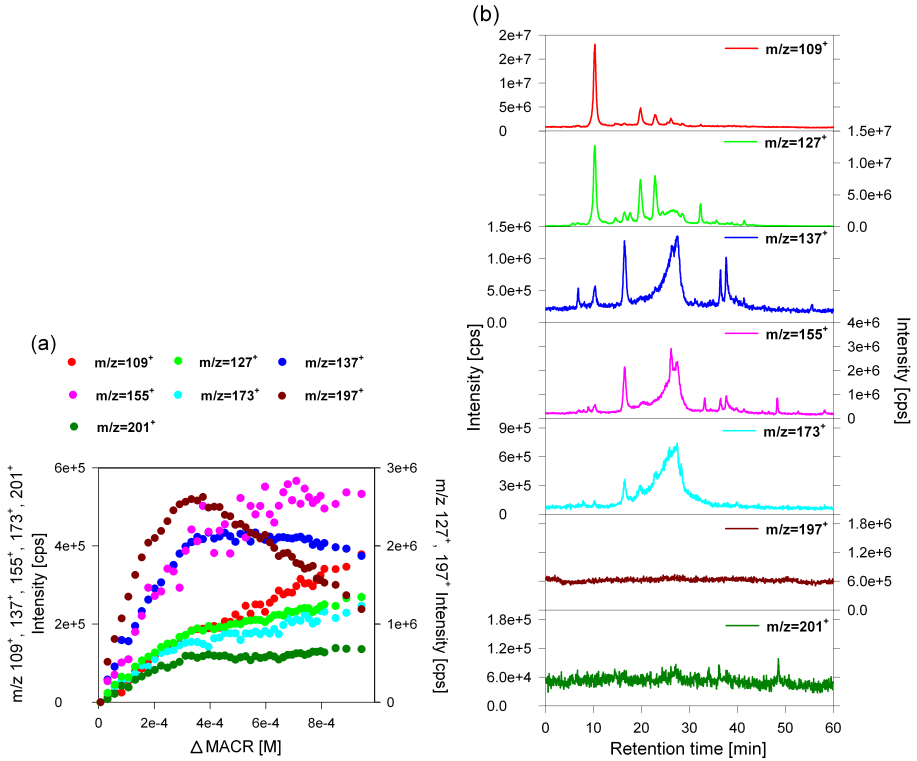

Fig. 5. Characteristics of the oligomer series B. **(a)** Evolution of the series B MS fragments intensities. The *m/z* 127^+ and 197^+ are plotted on the secondary axe. **(b)** HPLC chromatographic profiles related to the different MS fragments.

ACPD
9, 6425–6449, 2009

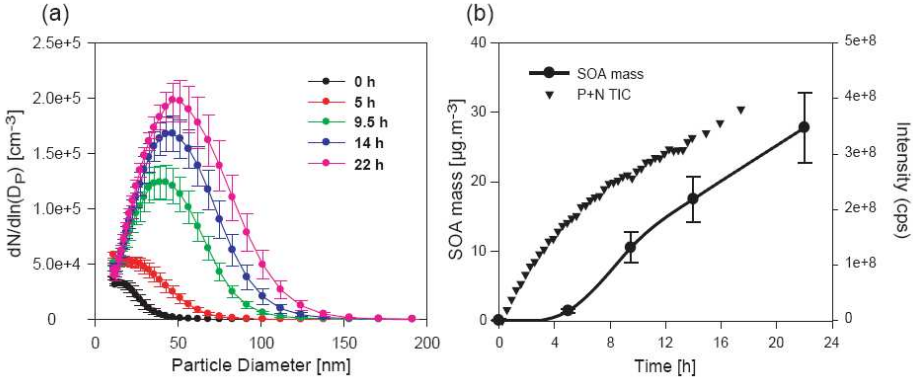

Fig. 6. **(a)** Evolution of the particles size number distributions of the generated SOA as a function of reaction time during the aqueous phase OH-oxidation of methacrolein. SOA was generated using the experimental setup described in Fig. 1. The particles number distributions of the generated SOA are an average of several distributions measured at the corresponding reaction times; the error bars represent the standard deviation of these averages. **(b)** The evolution of the SOA mass and the sum of the MS total ion current of the aqueous samples in the positive and the negative mode (P+N TIC) with the reaction time. The SOA mass are calculated using the SMPS data and assuming a particle density of 1 g cm^{-3}.

ACPD
9, 6425–6449, 2009